2021 43rd Annual International Conference of the
IEEE Engineering in Medicine & Biology Society (EMBC)
Oct 31 - Nov 4, 2021. Virtual Conference

Prototype and Evaluation of High-Hydrous Gel Phantom for 100 kHz to 1 MHz Using ATO/TiO2

S. Toyoda, *Student Member, IEEE*, T. Yamamoto, and K. Koshiji, *Member, IEEE*

Abstract— **This paper describes the development of a human electrical phantom in the low-frequency band. Conventional high-hydrous gel phantoms cannot mimic the electrical properties of the human body in the low-frequency band. Titanium oxide coated with antimony-doped tin oxide (ATO/TiO_2) was added to the high-hydrous gel phantom, and the electrical properties were evaluated in terms of the amount of material added. The developed phantom had an error of less than 10% in the range of 100 kHz to 1 MHz, which conforms with the electrical properties of human muscles. Particularly, at 125 kHz, the error was 2.71% and 4.35% for relative permittivity and conductivity, respectively. The variation in the electrical properties of the developed phantom was evaluated, and it was confirmed that sufficient reproducibility could be obtained.**

I. Introduction

Electromagnetic phantoms that mimic the electrical properties of a living body are widely used as substitutes for animals in experiments. Various types of phantoms have been developed, including liquid phantoms [1], [2], dry phantoms [3], and high-hydrous gel phantoms [4], [5]. The high-hydrous gel phantoms are easy to manufacture, have a high degree of freedom in shape, and are inexpensive to manufacture. This makes them useful in many applications. However, their electrical properties in the low-frequency band have not been well mimicked.

High-hydrous gel phantoms for the low-frequency band have been considered in various studies [6–9]. However, phantoms that mimic both relative permittivity and conductivity in the range of several hundred kHz have not yet been developed. For example, a transmission frequency of 100 kHz to 1 MHz (part of the study) is being considered in the transcutaneous energy transmission system (TETS), and phantoms are required to investigate the specific absorption rate [10], [11] and test the electromagnetic compatibility of the system [12], [13]. In addition, 125 kHz to 135 kHz is used for radio frequency identification (RFID) [14], and positioning systems require phantoms to account for disturbances caused by the living body. In this paper, we propose a new addition of ATO/TiO_2 [15], [16] to a high-hydrous gel phantom to improve its electrical properties. The changes in the electrical properties owing to the addition of ATO/TiO_2 were evaluated in terms of the material added. As a basic study, a high-hydrous gel phantom for 100 kHz to 1 MHz was developed. In addition, the reproducibility of the phantom was evaluated by measuring the variation in the electrical properties.

II. Electrical Properties of Human Muscle and Conventional Phantoms

In the low-frequency band around 1 MHz, biological tissues exhibit a steep change in electrical properties (β-dispersion) because of interfacial polarization caused by the cellular structure. Interfacial polarization occurs at heterogeneous parts of materials (i.e., interfaces with different electrical properties). Therefore, it is difficult to mimic β-dispersion using only basic materials of high-hydrous gel phantoms (e.g., deionized water, agar, sodium chloride, polyethylene powder, and TX-151). Previous studies have shown that the addition of carbon-based particles (e.g., carbon microcoils, carbon fibers, and active carbon fibers) to high-hydrous gel phantoms can improve the electrical properties in the low-frequency band [7–9]. This improvement is explained by interfacial polarization between water and the carbon-based particles owing to their high conductivity. However, because of the high conductivity of carbon-based particles, the conductivity of the phantom increases more than necessary, as shown in Fig. 1, making it difficult to mimic both relative permittivity and conductivity. Hence, it is necessary to decrease the conductivity of the particles. However, it is difficult to mimic the relative permittivity because the reduced conductivity of the particles decreases the dielectric relaxation intensity at the interfacial polarization.

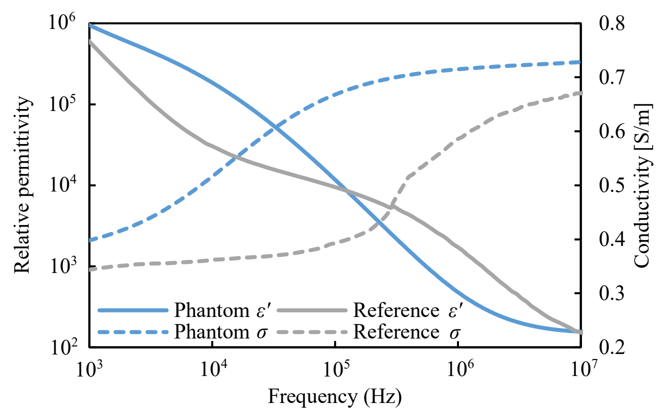

Fig. 1 Electrical properties of conventional phantom.

*Research supported by JSPS KAKENHI Grant Number 20K12631.

S. Toyoda, T. Yamamoto, K. Koshiji are with the Department of Electrical Engineering, Graduate school of Science and Technology, Tokyo University of Science, Chiba, Japan (phone: +81-4-7124-1501; fax: +81-4-7120-1741; e-mail: t_yamamoto@rs.tus.ac.jp).

The needle-shaped ATO/TiO_2 (ISHIHARA SANGYO KAISHA, LTD., FT-3000, Osaka, Japan) proposed in this paper as particles for inducing interfacial polarization has a conductivity, several orders of magnitude lower than that of carbon-based particles, and a relative permittivity exceeding 110. Therefore, the use of ATO/TiO_2 instead of carbon-based particles is assumed to decrease the conductivity while preventing a decrease in the dielectric relaxation intensity. In addition, ATO/TiO_2 is easily available because it is sold by many manufacturers.

III. Measurement Method

The two-electrode method was used to measure the electrical properties of the samples. The sample was held in acrylic (diameter 19 mm, height 16 mm) and sandwiched between a pair of silver/silver chloride electrodes (diameter 8.5 mm) and considered to be a parallel circuit of conductance G and capacitance C (see Fig. 2). The samples were measured using an LCR meter (NF corporation, ZM2376, Kanagawa, Japan), and the relative permittivity ε' and conductivity σ were calculated using (1) and (2).

$$\varepsilon' = \frac{Cd}{\varepsilon_0 S} \quad (1)$$

$$\sigma = \frac{Gd}{S} \quad (2)$$

where d, S, and ε_0 denote the distance between the parallel plates, electrode area, and vacuum permittivity (8.854×10^{-12} F/m), respectively.

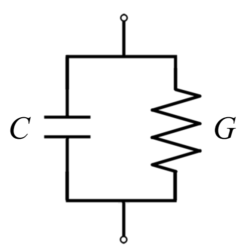

Fig. 2 Equivalent circuit for measurement.

IV. Evaluation of Electrical Properties

A. Change in the amount of material added

Figs. 3 and 4 demonstrate the electrical properties of the phantom when the amount of ATO/TiO_2 is changed according to Table I (i). By increasing the amount of ATO/TiO_2, the dielectric relaxation intensity and high-frequency limiting value of the relative permittivity increased, and the dielectric relaxation frequency shifted to the high-frequency side. In addition, the low-frequency limiting value of conductivity does not increase linearly with an increase in the amount of ATO/TiO_2 added, but converges to a certain value.

Figs. 5 and 6 demonstrate the electrical properties when the amount of sodium chloride is changed according to Table I (ii). The increase in conductivity and the shift of the dielectric relaxation frequency to the high-frequency side were confirmed by increasing the amount of sodium chloride added. When the mass of the added sodium chloride is 0.07 g, the dielectric relaxation intensity decreased because of the smaller difference in conductivity between water and ATO/TiO_2.

Table I Composition of the phantom with varying addition amount

Material	**Addition amount (g)**	
	(i)	**(ii)**
Deionized water	183.95–191.95	183.93–183.97
Agar	6.00	6.00
Sodium chloride	0.05	0.03–0.07
ATO/TiO_2	2.00–10.00	10.00
Total	200.00	200.00

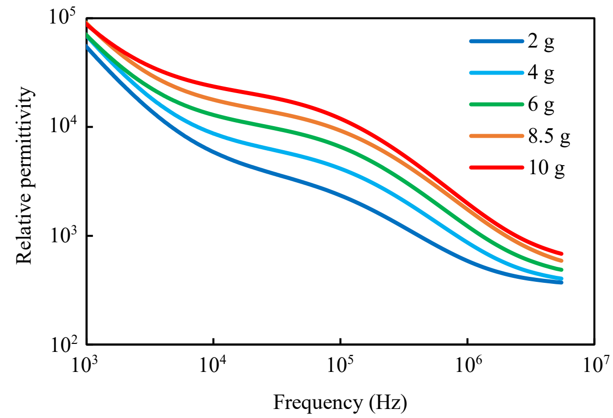

Fig. 3 Relative permittivity with varying ATO/TiO_2 addition.

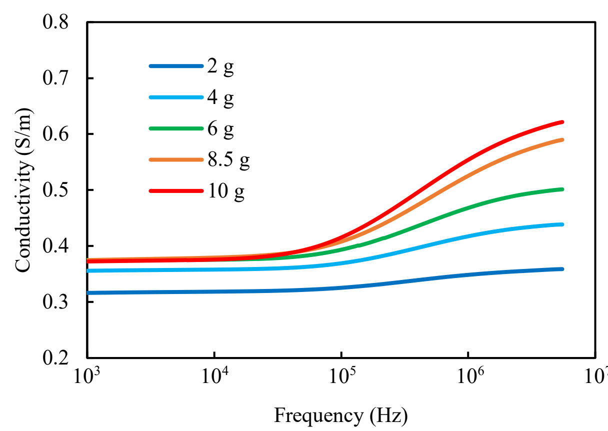

Fig. 4 Conductivity with varying ATO/TiO_2 addition.

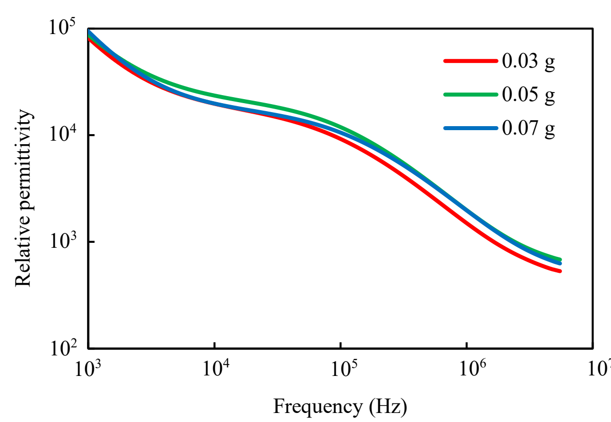

Fig. 5 Relative permittivity with varying sodium chloride addition.

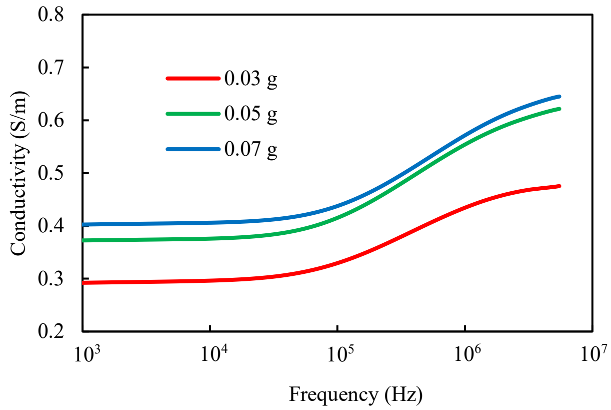

Fig. 6 Conductivity with varying sodium chloride addition.

B. *Electrical properties in target frequency*

The relationship between the relative permittivity and conductivity at 125 kHz with varying amounts of ATO/TiO_2 and NaCl is shown in Fig. 7. For the target value, we used the electrical properties of the human muscle measured by Gabriel et al. [16], [17]. The relative permittivity and conductivity increased linearly with increasing amounts of ATO/TiO_2 and sodium chloride, respectively. With the increase in the amount of ATO/TiO_2 added, the conductivity increased slowly and approached a constant value. The partial increase in the relative permittivity with the increase in the amount of sodium chloride added is due to the shift of the dielectric relaxation frequency to the high-frequency side. However, the decrease in relative permittivity with an increase in the amount of sodium chloride added is due to the decrease in the dielectric relaxation intensity. The region surrounded by the plot points depicted in Fig. 7 can be mimicked by the phantom. Because the electrical properties of human muscle are contained within the region, it can be mimicked by adjusting the amount of material added. The relative error showed the minimum value when 9.20 g of ATO/TiO_2 and 0.05 g of sodium chloride were added, which was 2.71% for the relative permittivity and 4.35% for the conductivity.

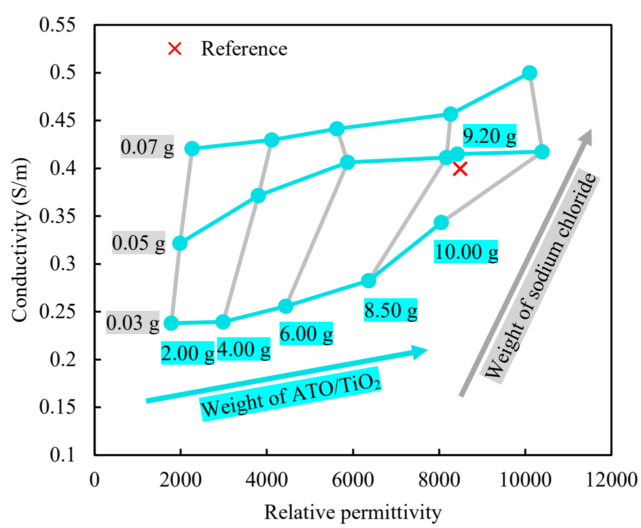

Fig. 7 Adjustment of electrical properties of phantom at 125 kHz.

V. Prototype of The Phantom

A. *Mimic the electrical properties of human muscle*

Using the confirmed changes in the electrical properties obtained in Fig. 7, a prototype of the phantom was examined at the set target frequency band of 100 kHz to 1 MHz. The phantom was prototyped based on the composition shown in Table II. The electrical properties of the ATO/TiO_2-added phantom are illustrated in Fig. 8. The average relative errors between 0.1 MHz and 1 MHz were −1.70% and 3.45% for the relative permittivity and conductivity, respectively. The maximum relative errors were −8.54% for relative permittivity at 0.4 MHz and 9.33% for conductivity at 0.9 MHz. The reference value of the electrical properties is unnaturally increased at approximately 0.3 MHz (probably because of measurement errors); thus, the error is actually small. Therefore, because the error is within 10% in the target frequency band, it conforms with the electrical properties of the human muscle.

Table II Composition of prototype phantom

Material	Addition amount [g]
Deionized water	184.75
Agar	6.00
Sodium chloride	0.05
ATO/TiO_2	9.20

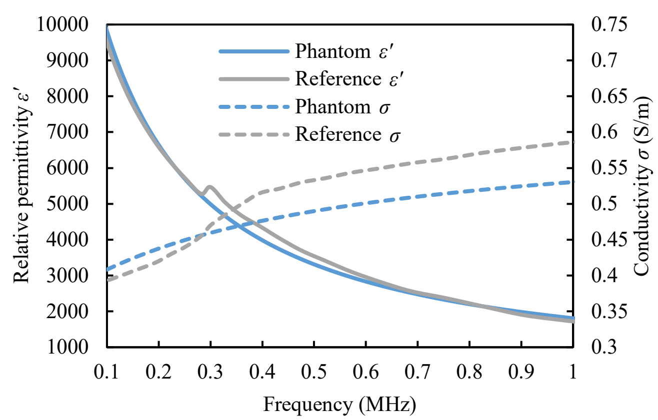

Fig. 8 Electrical properties of ATO/TiO_2-added phantom.

B. *Evaluation of variation in electrical properties*

Because the ATO/TiO_2-added phantom has a heterogeneous structure and the electrical properties are easily varied, the reproducibility of the electrical properties was evaluated. Table III shows the variation in electrical properties at 125 kHz when five phantoms were fabricated per time, for a total of three times. The standard deviation of each time indicates the variation of electrical properties from place to place, and the total standard deviation indicates the variation of electrical properties from prototype to prototype. Although the variation in electrical properties from prototype to prototype is small, the variation in electrical properties from place to place is large. This variation is believed to be attributable to the agglomeration of particles and is expected to be improved by the addition of dispersants.

Table III Variation of electrical properties at 125 kHz

	Average		Standard deviation	
	ε'	σ (S/m)	ε'	σ (S/m)
First	8805	0.4237	254.4	0.01533
Second	8062	0.3921	440.3	0.02510
Third	8425	0.4149	737.9	0.04131
Total	8431	0.4102	599.8	0.03216

VI. CONCLUSION

In this paper, we proposed a method to mimic the electrical properties of a living body in the low-frequency band by adding ATO/TiO_2 to a conventional high-hydrous gel phantom. We avoided the excessive increase in conductivity, which was an issue in previous studies, by using ATO/TiO_2 and were able to bring the electrical properties in the low-frequency band closer to the reference values. In addition, the change in electrical properties in terms of material addition was considered, and an ATO/TiO_2-added phantom usable from 100 kHz to 1 MHz was fabricated. We confirmed that the system can mimic the electrical properties of the human muscle in the target frequency band with an error of less than 10%. In particular, at 125 kHz, the relative errors were 2.71% and 4.35% for relative permittivity and conductivity, respectively. Although the variation in electrical properties from prototype to prototype was small, the electrical properties from place to place varied owing to particle agglomeration. This variation is expected to be improved by adding dispersants. In the future, we can create phantoms that can mimic more accurately over a wider frequency band by using polyethylene powder and TX-151 to reduce the relative permittivity of water.

REFERENCES

[1] M. I. Khattak, R. M. Edwards and J. Ma, "A study of perturbations due to antennas in close proximity with the human body and body simulating liquid filled phantoms at 1.8 GHz," *Loughborough Antennas & Propagation Conference*, pp. 625–628, 2009.

[2] J. Chakarothai, K. Wake, L. Hamada and S. Watanabe, "SAR evaluation using human-equivalent liquid phantom in wireless power transfer frequency band," *2015 International Workshop on Electromagnetics: Applications and Student Innovation Competition*, pp. 1–2, 2015.

[3] T. Kobayashi, T. Nojima, K. Yamada and S. Uebayashi, "Dry phantom composed of ceramics and its application to SAR estimation," *IEEE Transactions on Microwave Theory and Techniques*, vol. 41, no. 1, pp. 136–140, 1993.

[4] K. Ito, Y. Okano, A. Hase, T. Asahina and H. Yoshimura, "A study on solid phantoms for estimation of interaction between human body and electromagnetic waves," *1999 International Symposium on Electromagnetic Compatibility*, pp. 337–340, 1999.

[5] C. K. Chou, G. W. Chen, A. W. Guy and K. H. Luk, "Formulas for preparing phantom muscle tissue at various radiofrequencies," *Bio electromagnetics*, vol. 5, no. 4, pp. 435–441, 1984.

[6] L. Fomundam and J. Lin, "Multi-layer low frequency tissue equivalent phantoms for noninvasive test of shallow implants and evaluating antenna-body interaction," *2016 38th Annual International Conference of the IEEE Engineering in Medicine and Biology Society*, pp. 2353–2356, 2016.

[7] T. Yamamoto, K. Sano, K. Koshiji, X. Chen, S. Yang, M. Abe and A. Fukuda, "Development of electromagnetic phantom at low-frequency band," *2013 35th Annual International Conference of the IEEE Engineering in Medicine and Biology Society*, pp. 1887–1890, 2016.

[8] T. Yamamoto, R. Ikeda, D. Yamada, A. Saitoh and K. Koshiji, "Development of a high-hydrous gel phantom for human body communication based on electrical anisotropy," *2019 41st Annual International Conference of the IEEE Engineering in Medicine and Biology Society*, pp. 4028–4031, 2019.

[9] S. Toyoda, T. Yamamoto and K. Koshiji, "Improvement of electrical properties of high-hydrous gel phantom at low frequency band using activated carbon fiber," *Journal of the Japan Society of Applied Electromagnetics and Mechanics*, vol. 28, no. 2, pp. 51–56, 2020.

[10] O. Knecht and J. W. Kolar, "Impact of transcutaneous energy transfer on the electric field and specific absorption rate in the human tissue," *41st Annual Conference of the IEEE Industrial Electronics Society*, pp. 4977–4983, 2015.

[11] K. Shiba, N. E. B. Zulkiffi and Y. Ishioka, "Analysis of specific absorption rate and internal electric field in human biological tissues surrounding an air-core coil-type transcutaneous energy transmission transformer," *Journal of Artificial Organs*, vol. 20, pp. 103–109, 2017.

[12] Y. Wu, A. P. Hu, D. Budgett, S. Malpas and T. Dissanayake, "Harmonic analysis of voltage-fed full-bridge converter for TET application," *2010 5th IEEE Conference on Industrial Electronics and Applications*, pp. 1040–1045, 2010.

[13] T. Campi, S. Cruciani, F. Maradei, A. Montalto, F. Musumeci and M. Feliziani, "EMI in a cardiac implantable electronic device (CIED) by the wireless powering of a left ventricular assist device (LVAD)," *IEEE Transactions on Electromagnetic Compatibility*, pp. 1–8, 2020.

[14] V. Gharat, E. Colin, G. Baudoin and D. Richard, "Indoor performance analysis of LF-RFID based positioning system: Comparison with UHF-RFID and UWB," *2017 International Conference on Indoor Positioning and Indoor Navigation*, pp. 1–8, 2017.

[15] X. Li, J. Qian, J. Li, J. Xu, J. Xing and L. Liu, "A facile synthesis of antimony-doped tin oxide-coated TiO_2 composites and their electrical properties," *Journal of Materials Science: Materials in Electronics*, vol. 30, pp. 9289–9302, 2019.

[16] Z. Chen, M. Gu, F. Wang, C. Gao, P. Liu, Y. Ding, S. Zhang and M. Yang, "Conductive TiO_2 nanorods via surface coating by antimony doped tin dioxide," *Materials Chemistry and Physics*, vol. 225, pp. 181–186, 2019.

[17] S. Gabriel, R. W. Lau and C. Gabriel, "The dielectric properties of biological tissues: II. Measurements in the frequency range 10 Hz to 20 GHz," *Physics in Medicine & Biology*, vol. 41, no. 11, pp. 2251–2269, 1996.